COMMUNICATION

Light Absorption Enhancement in Thin-Film Solar Cells Using Whispering Gallery Modes in Dielectric Nanospheres

Jonathan Grandidier, Dennis M. Callahan, Jeremy N. Munday, and Harry A. Atwater*

For thin-film solar cells, light absorption is usually proportional to the film thickness. However, if freely propagating sunlight can be transformed into a guided mode,[1] the optical path length significantly increases and results in enhanced light absorption within the cell.[2] We propose here a light absorber based on coupling from a periodic arrangement of resonant dielectric nanospheres. It is shown that whispering gallery modes in the spheres can be coupled into particular modes of the solar cell and significantly enhance its efficiency. We numerically demonstrate this enhancement using full-field finite difference time-domain (FDTD) simulations of a nanosphere array above a typical thin-film amorphous silicon (a-Si) solar cell structure. The in-coupling element in this design is advantageous over other schemes as it is composed of a lossless material, and its spherical symmetry naturally accepts large angles of incidence. Also, the array can be fabricated using simple, well-developed methods of self assembly and is easily scalable without the need for lithography or patterning. This concept can be easily extended to many other thin-film solar cell materials to enhance photocurrent and angular sensitivity.

Thin-film photovoltaics offer the potential for a significant cost reduction[3] compared to traditional, or first generation, photovoltaics usually at the expense of high efficiency. This is achieved mainly by the use of amorphous or polycrystalline optoelectronic materials for the active region of the device, for example, a-Si. The resulting carrier collection efficiencies, operating voltages, and fill factors are typically lower than those for single-crystal cells, which reduce the overall cell efficiency. There is thus great interest in using thinner active layers combined with advanced light trapping schemes to minimize these problems and maximize efficiency. A number of light trapping schemes have been proposed and demonstrated including the use of plasmonic gratings,[4,5] arrays of metal cavities that support void plasmons,[6] photonic crystals,[7] nano- and microwires,[8,9] nanodomes,[10] aggregates of nanocrystallites,[11] and dielectric diffractive structures.[12] A previous report[12] described the use of sub-wavelength dielectric spheres and other scattering mechanisms for enhancing light scattering and absorption. Here, we propose a new concept for light trapping in thin-film solar cells through the use of wavelength-scale resonant dielectric nanospheres that support whispering gallery modes to enhance absorption and photocurrent.

Wavelength-scale dielectric spheres[13] are interesting photonic elements because they can diffractively couple light from free space and also support confined resonant modes. Moreover, the periodic arrangement of nanospheres can lead to coupling between the spheres, resulting in mode splitting and rich bandstructure.[14,15] The coupling originates from whispering gallery modes (WGM) inside the spheres.[15,16] When resonant dielectric spheres are in proximity to a high-index photovoltaic absorber layer, incident light can be coupled into the high-index material and can increase light absorption. Another important benefit of this structure for photovoltaic application is its spherical geometry that naturally accepts light from large angles of incidence.

Figure 1a depicts a solar cell where close packed dielectric resonant nanospheres stand atop a typical a-Si solar cell structure. A cross section is represented in Figure 1c. We use a silver back contact and, in order to avoid diffusion between the silver layer and the a-Si layer, a 130-nm aluminium-doped zinc oxide (AZO) layer is placed between the silver and the a-Si layer.[17] An 80-nm indium tin oxide (ITO) layer is used as a transparent conducting front contact and also acts as an antireflection coating. 600-nm-diameter silica nanospheres with a refractive index of $n = 1.46$ are directly placed on the ITO as a hexagonally close-packed monolayer array. In order to study the response of the system, we performed 3D full field electromagnetic simulations to determine the expected absorption enhancement compared to a-Si absorbers without a layer of dielectric spheres. A broadband wave pulse with the electric field polarized along the x-axis (see Figure 1a) is injected at normal incidence on the structure, and the fields are monitored at 100 wavelengths equally spaced between $\lambda = 300$ nm and $\lambda = 800$ nm. This wavelength range corresponds to the sun's energy spectrum below the bandgap of a-Si. In order to determine how much current can be generated from the structure, we calculated the optical generation rate in the silicon using[18]

$$G_{opt}^{n}(\omega) = \int \frac{\varepsilon''(\omega)|E(\omega)|_S^2}{2\hbar} \Gamma_{solar}(\omega) \, dV \tag{1}$$

where ω is the angular frequency, $\hbar$ is Planck's constant divided by 2π, $\varepsilon''(\omega)$ is the imaginary part of the dielectric function of the silicon, and $|E(\omega)|_S^2$ is the electric field intensity integrated over the simulation volume containing the amorphous silicon.[19] If all electrons generated are collected, this will correspond to the device's current. Γ_{solar} is a factor used to weight each wavelength by the AM1.5 solar spectrum. In Figure 1d, we plot the normalized integrated electric field and absorption of a cross section at the center of the sphere perpendicular to the incoming plane wave and in the plane of the electric field

Dr. J. Grandidier, D. M. Callahan, Dr. J. N. Munday, Prof. H. A. Atwater
Thomas J. Watson Laboratories of Applied Physics
California Institute of Technology
Pasadena, CA 91125, USA
E-mail: jgrandid@caltech.edu

Materials
Views
www.MaterialsViews.com

ADVANCED
MATERIALS
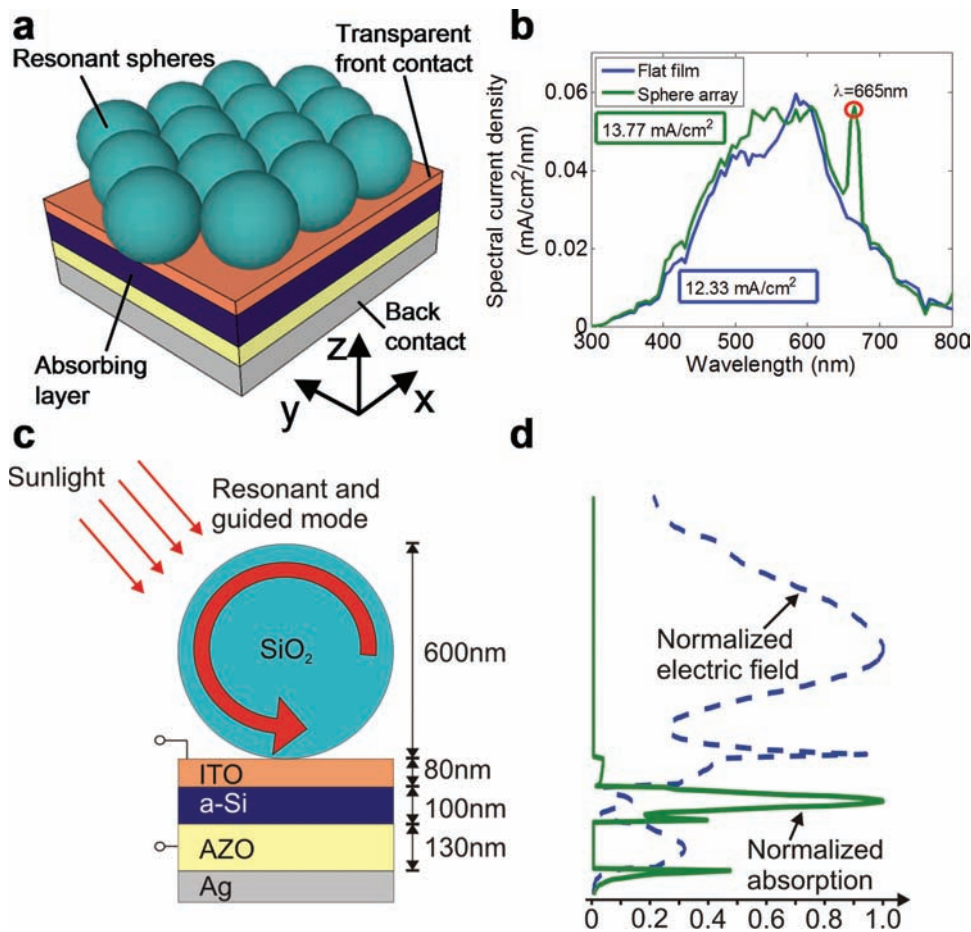www.advmat.de

COMMUNICATION

Figure 1. a) Schematic of the dielectric nanosphere solar cell. b) Current density calculated in the amorphous silicon layer with and without the presence of nanospheres. The a-Si thickness is 100 nm and the sphere diameter is $D = 600$ nm. c) Cross section of a silica nanosphere on an amorphous silicon layer with an AZO and silver back contact layer. d) Integrated electric field and absorption calculated from Figure 2a for normal incidence of a cross section at the center of the sphere at the resonant frequency corresponding to $\lambda = 665$ nm.

for the resonant frequency corresponding to $\lambda = 665$ nm. The absorption is proportional to $\varepsilon''(\omega)|E(\omega)|^2{}_S$ as shown in Equation 1.

To determine the influence of the spheres on the solar cell structure presented in Figure 1a, we calculate the spectral current density in the a-Si layer with and without the presence of 600-nm-diameter nanospheres. The result is presented in Figure 1b. The overall integrated current density corresponding to the energy absorbed in the a-Si in the presence of the nanospheres is $J = 13.77$ mA cm^{-2}, which corresponds to an enhancement of 12% compared to the case without the sphere array. Over almost the entire wavelength range, the spectral current density is higher with the spheres than without the spheres. Furthermore, discrete enhancements at specific wavelengths exist due to coupling between the spheres and the solar cell. The broadband enhancement can be explained by the spheres acting as a textured antireflection coating. At $\lambda = 665$ nm, the enhancement is greater than 100%. To explain this increase in the current density, we plot in **Figure 2**a the electric field intensity for a cross section in the middle of a sphere in the (x,z)-plane. Two lobes are observed on each side of the sphere. These are

characteristic of WGMs. They have significant field strength within the periodic arrangement of the sphere layer.

The WGMs of the spheres couple with each other due to their proximity,[20] which can lead to waveguide formation.[14] A planar waveguide mode can be formed by a 1D chain [21] of touching spheres and has been termed as a "nanojet" mode;[22] in our case, we are simply extending this to two dimensions.

We represent in Figure 2b,c the E_y component of the electric field for a cross section in the (x,y)-plane in the middle of the a-Si layer. The observed field profile is periodic and oscillates in phase with the period. Because the sphere array by itself has very low loss, the mode energy eventually gets absorbed into the a-Si and increases the generated photocurrent. In Figure 2c, we show the E_y component of the electric field, corresponding to a transverse electric (TE) guided mode along the x-axis. There also exists a transverse magnetic (TM) guided mode of the same periodicity that contributes to the enhancement of the absorption at $\lambda = 665$ nm (not shown). As a comparison, we show in Figure 2d–f an equivalent analysis, off resonance at $\lambda = 747$ nm. Clearly there is no resonance in the sphere and no excitation of a guided mode at this wavelength.
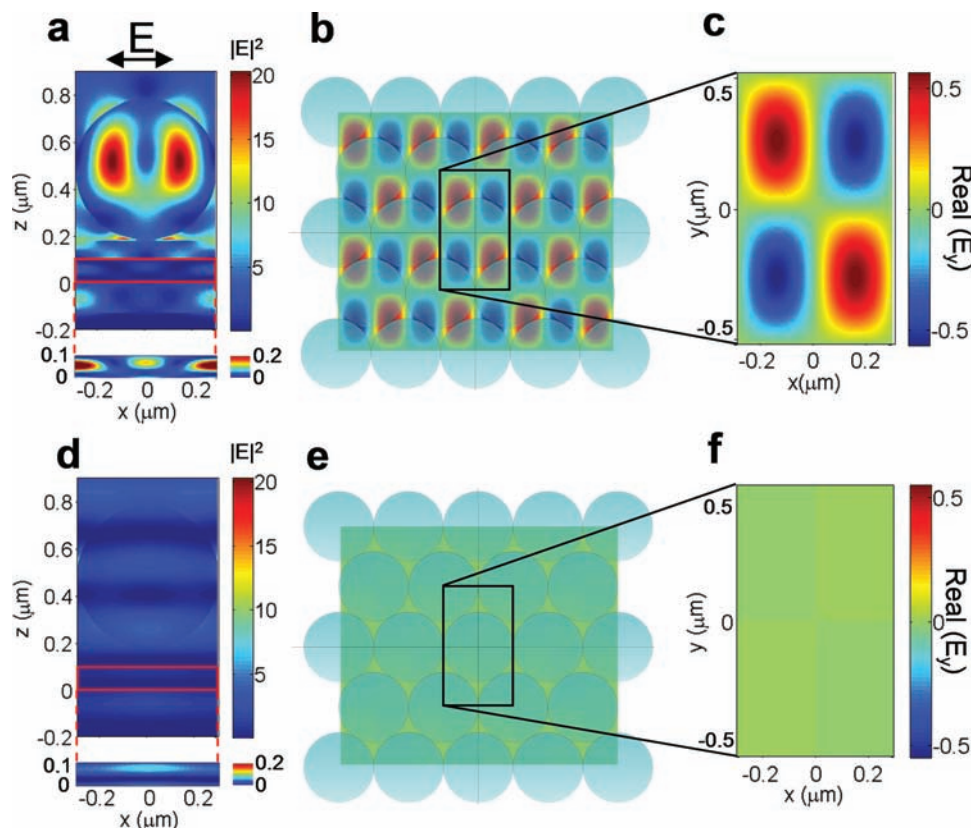
Figure 2. a) Electric field intensity for a cross section at the middle of a sphere in the (x,z)-plane at $\lambda = 665$ nm. Below is an enlargement of the a-Si layer. The direction of the electric field of the incident plane wave is also represented. b,c) E_y component of the electric field from a cross section in the (x,y)-plane in the middle of the a-Si layer. d–f) Same as (a–c) for $\lambda = 747$ nm, which corresponds to a frequency off resonance.

The spherical shape of the structure above the solar cell also enables incoupling at large angles of incidence. In order to verify this, we compared the absorbed light at normal incidence and at 20° and 40° angle to the normal in both TE and TM polarizations. For simplicity, we considered only an array of silica spheres above a 100-nm a-Si layer. **Figure 3**a,d show a schematic of the simulated structures without and with silica spheres on top of the a-Si. Figure 3b,c and e,f correspond to the spectral current density in the a-Si for both cases without and with silica spheres, respectively, and for TE and TM polarizations. For normal incidence, the calculated improvement is 29.6% and is independant of the polarization. This high improvement compared to the solar cell previously described can be explained by the absence of an antireflection coating layer and back reflector layer in this simplified case. For TM polarization, the improvement is 13.8% for 20° and 3.9% for 40° incidence angle. For TE polarization, the improvement compared to a flat layer remains around 29% for all angles. However, in the case of a flat a-Si film with incident TM polarization, the larger the angle, the larger the energy absorbed. That is why the current improvement of a structure with spheres decreases over that of a structure without spheres in the case of a TM-polarized incident plane wave.

As the lattice constant Λ of the hexagonal array of spheres varies, as represented in Figure 3g, the absorption due to the

WGM-guided wave changes due to different coupling conditions between the spheres. In Figure 3h, we show the spectral current density for different spacings between the spheres. The peak at $\lambda = 665$ nm for close-packed spheres is shifted to longer wavelengths as the distance between the spheres increases. This provides evidence that the incoupling is due to a diffractive mechanism. For $\Lambda = 650$ nm and $\Lambda = 700$ nm, a second peak appears at $\lambda = 747$ nm and $\lambda = 780$ nm, respectively. This corresponds to an optimal coupling condition between the WGM and the a-Si waveguide mode for these specific periodicities and wavelengths. For the considered design, a separation of $\Lambda = 700$ nm gives the highest current density with $J = 14.14$ mA cm^{-2}, which represents an enhancement of 15% compared to a flat a-Si cell with an antireflection coating. As shown in Figure 3i, when $\Lambda > 1000$ nm, the coupling between the spheres almost disappears and the enhancement significantly decreases. From an experimental point-of-view, the spacing between spheres could be varied by an additional coating on each sphere or by assembly on photolithographically patterned substrates.[23] An intriguing aspect of changing the spacing between the spheres is that it allows one to tune and adjust which wavelengths are coupled into the solar cell.

In order to estimate the influence of the sphere diameter on the enhancement of the solar cell efficiency, we illustrate in **Figure 4** the ratio between the spectral current density of a
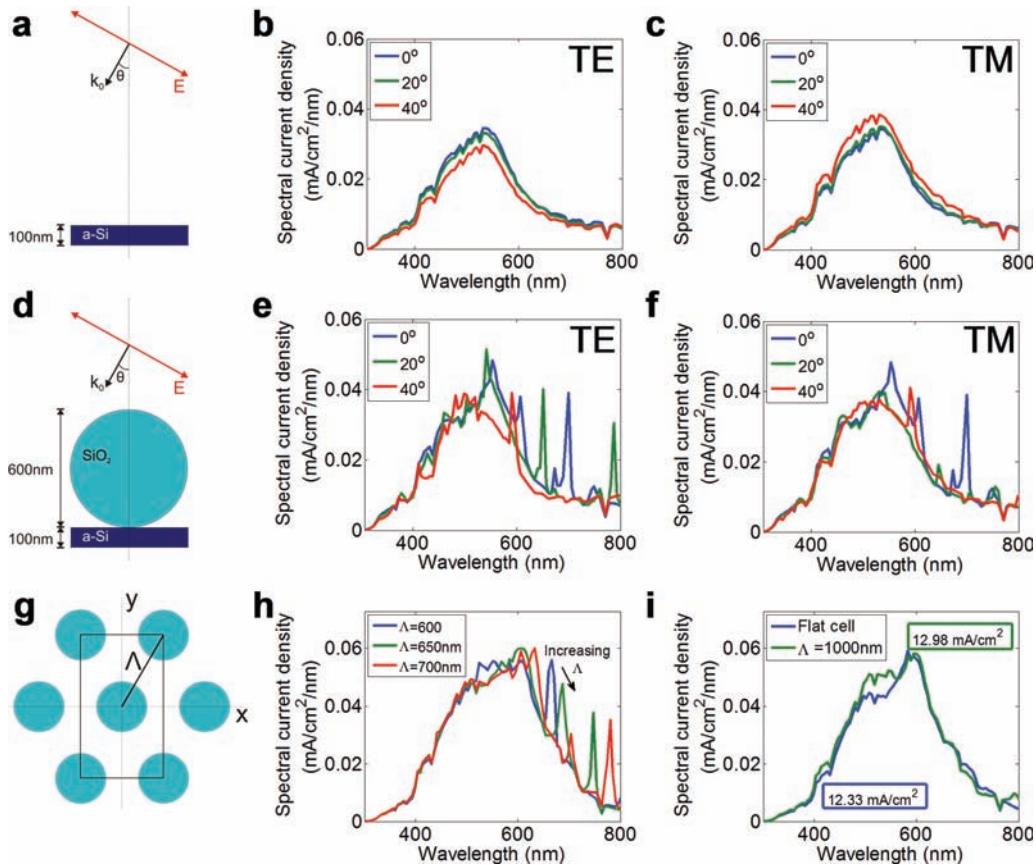
Materials
Views
www.MaterialsViews.com

ADVANCED
MATERIALS
www.advmat.de

COMMUNICATION

Figure 3. a) Schematic of the flat case model with an angle and spectral current density in b) TE and c) TM polarization. d) Schematic of the case with nanospheres on top and spectral current density in e) TE and f) TM polarization. g) Top view of the periodic arrangement of the nanospheres with a large lattice constant. The rectangle indicates the unit cell used for numerical simulations. h) Current density for three different sphere spacings when an efficient coupling between the spheres exists. i) Current density for a flat cell and with a relatively large distance between the spheres (Λ = 1000 nm).
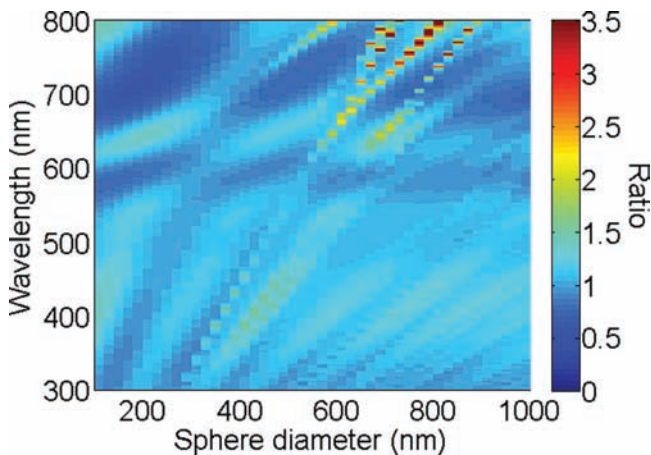

Figure 4. Ratio between the spectral current density of a solar cell with hexagonally close-packed spheres over the spectral current density of a solar cell without spheres.

solar cell with hexagonally close-packed spheres over the spectral current density of a solar cell without spheres. The sphere diameter varies between D = 100 nm and D = 1000 nm. We

again observe a general broadened enhancement due to the effective textured antireflection coating created by the layer of spheres. Moreover, strong enhancement occurs in Figure 4 corresponding to optical dispersion of the array of coupled whispering gallery mode dielectric spheres. We note that the effective dispersion curves in Figure 4 appear as arrays of bright dots; this is a plotting artifact arising from simulation at discrete sphere diameters spaced in increments of 20 nm; simulation at a finer sphere size resolution was not possible due the computational size of these 3D simulations. Because the a-Si absorption becomes weaker above λ = 600 nm, the enhancement corresponding to the WGMs becomes significant above this wavelength. This strong enhancement where a-Si is weakly absorbing is obtained for sphere diameters between 500 and 900 nm. Therefore, a way to broadly enhance the a-Si absorption in this weakly absorbing region could be to randomly mix sphere diameters in the range 500 to 900 nm.

We have investigated several photovoltaic absorber configurations based on a periodic array of resonant silica nanospheres atop an a-Si layer and demonstrated that strong whispering gallery modes can significantly increase light absorption in a-Si thin-film solar cells. We presented here a new concept for a solar cell where a resonant guided mode is excited due to a

COMMUNICATION

nanosphere array above the active layer and is eventually absorbed in the a-Si under it. We optimized the structure design for the largest absorption enhancement for a given sphere diameter. The spectral position of the absorption enhancement can be easily tuned by varying the sphere diameter and lattice constant. Also, the number of resonances can potentially be increased to make the response more broadband by assembling arrays of spheres with different diameters.[24] This concept has advantages over other absorption enhancement schemes because the incoupling elements are lossless and their spherical geometry allows light to be efficiently coupled into the solar cell over a large range of incidence angles. Also these arrays can be fabricated and easily scaled using standard self-assembly[16,25] techniques without the need for lithography. In addition to this, the presented enhancement results are performed on a totally flat a-Si layer, which has an advantage over cells grown on textured surfaces as surface roughness or topography can create holes or oxidation and thus reduce the efficiency and lifetime of the solar cell. The sphere array can also be easily integrated or combined with existing absorption enhancement techniques. This light trapping concept offers great flexibility and tunability and can be extended for use with many other thin-film solar cell materials.

[1] P. N. Saeta, V. E. Ferry, D. Pacifici, J. N. Munday, H. A. Atwater, *Opt. Express* **2009**, *17*, 20975.

[2] E. Yablonovitch, G. D. Cody, *IEEE Trans. Electron Dev.* **1982**, **ED-29**, 300.

[3] H. A. Atwater, A. Polman, *Nat. Mater.* **2010**, *9*, 205.

[4] J. N. Munday, H. A. Atwater, *Nano Lett.* **2010**, DOI: 10.1021/nl101875t.

[5] R. A. Pala, J. White, E. Barnard, J. Liu, M. L. Brongersma, *Adv. Mater.* **2009**, *21*, 3504.

[6] T. V. Teperik, F. J. García de Abajo, A. G. Borisov, M. Abdelsalam, P. N. Bartlett, Y. Sugawara, J. J. Baumberg, *Nat. Photonics* **2008**, *2*, 299; and reference cited therein.

[7] P. Bermel, C. Luo, L. Zeng, L. C. Kimerling, J. D. Joannopoulos, *Opt. Express* **2007**, *15*, 16986.

[8] M. D. Kelzenberg, S. W. Boettcher, J. A. Petykiewicz, D. B. Turner-Evans, M. C. Putnam, E. L. Warren, J. M. Spurgeon, R. M. Briggs, N. S. Lewis, *Nat. Mater.* **2010**, *9*, 239.

[9] E. Garnett, P. Yang, *Nano Lett.* **2010**, *10*, 1082.

[10] J. Zhu, C.-M. Hsu, Z. Yu, S. Fan, Y. Cui, *Nano Lett.* **2010**, *10*, 1979.

[11] Q. F. Zhang, T. R. Chou, B. Russo, S. A. Jenekhe, G. Z. Cao, *Angew. Chem., Int. Ed.* **2008**, *47*, 2402.

[12] M. Kroll, S. Fahr, C. Helgert, C. Rockstuhl, F. Lederer, T. Pertsch, *Phys. Status Solidi A* **2008**, *205*, 2777.

[13] Y. Xia, B. Gates, Y. Yin, Y. Lu, *Adv. Mater.* **2000**, *12*, 693.

[14] A. Yariv, Y. Xu, R. K. Lee, A. Scherer, *Opt. Lett.* **1999**, *24*, 711–713.

[15] R. M. Cole, Y. Sugawara, J. J. Baumberg, S. Mahajan, M. Abdelsalam, P. N. Bartlett, *Phys. Rev. Lett.* **2006**, *97*, 137401.

[16] X. Yu, L. Shi, D. Han, J. Zi, P. V. Braun, *Adv. Funct. Mater.* **2010**, *20*, 1910.

[17] V. E. Ferry, M. A. Verschuuren, H. B. T. Li, E. Verhagen, R. J. Walters, R. E. I. Schropp, H. A. Atwater, A. Polman, *Opt. Express* **2010**, *18*, 237.

[18] V. E. Ferry, J. N. Munday, H. A. Atwater, *Adv. Mater.* **2010**, *22*, 4794.

[19] A. D. Yaghjian, *IEEE Trans. Antennas Propag.* **2007**, *55*, 1495.

[20] A. N. Oraevsky, *Quantum Electron.* **2002**, *32*, 377–400.

[21] T. Mitsui, Y. Wakayama, T. Onodera, T. Hayashi, N. Ikeda, Y. Sugimoto, T. Takamasu, H. Oikawa, *Adv. Mater.* **2010**, *22*, 3022.

[22] Z. Chen, A. Taflove, V. Backman, *Opt. Lett.* **2006**, *31*, 389.

[23] Y. Yin, Y. Lu, B. Gates, Y. Xia, *J. Am. Chem. Soc.* **2001**, *123*, 8718.

[24] V. Kitaev, G. A. Ozin, *Adv. Mater.* **2003**, *15*, 75.

[25] M. Bardosova, M. E. Pemble, I. M. Povey, R. H. Tredgold, *Adv. Mater.* **2010**, *22*, 3104.